Temperature Measurements of Laminar Propane/Air Premixed Flame Using Detailed OH* Spectra Intensity Ratio

by

Y. Ikeda[(1)] , T. Kurahashi[(2)], N. Kawahara[(2)] and E. Tomita[(2)]

[(1)] Imagineering, Inc.
Welv Rokko 2nd Bldg. 5F 4-1-1 Fukada, Nada, Kobe 657-0038 JAPAN
[(2)] Okayama University
Department of Mechanical Engineering,
Tsushima-Naka 3, Okayama 700-8530; Japan
[(1)]E-Mail: yuji@imagineering.jp

ABSTRACT

The spatially resolved chemiluminescence at the flame front and anchor point of a laminar premixed propane/air flame was measured in this study. The flame front structure, anchor point location, and local equivalence ratio were examined for different values of the equivalence ratio f ranging from 0.9 to 1.5 using the chemiluminescence spectra. Local point-measurements of the chemiluminescence were obtained using a developed Cassegrain optics system, which had a spatial resolution of d = 0.08 mm and L = 0.6 mm, sufficient to measure the detailed location of the anchor point and the flame front shape. The anchor point was not in the same location for different values of f. The lower anchor point was located 0.3 mm above the rim and at a radial distance of 6.8 mm when f = 1.0, 1.1, and 1.2, and the anchor point location trace was a V shape. The equivalence ratio of the anchor point was calculated from the relationship of the OH*/CH* intensity and the local equivalence ratio, and the measured value was constant for different values of f. The detailed OH* and CH* spectra demonstrated that the chemistry at the anchor point was dominated by the same processes for different equivalence ratios. The local equivalence ratio at the anchor point was between 0.7 and 0.8 for all experimental conditions. The temperature at the anchor point was estimated using the detailed OH* R and P branch intensity ratio used for plasma diagnostics. The results indicate that the temperature at the flame front was relatively constant, although the temperature at the anchor point showed remarkable changes that could be predicted from the heat loss.

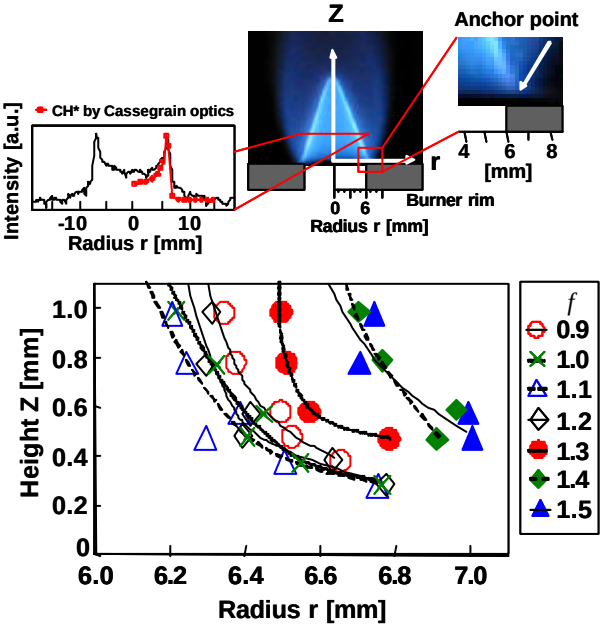

Fig. 7 Flame front location and anchor point for different equivalence ratio

1. INTRODUCTION

Flame stabilization is an essential subject that requires investigation. It must be carefully controlled when using a combustion apparatus, and is affected by recirculation, mixing, and diffusion. There have been many reports written about flame holding mechanisms, and the detailed stabilization mechanisms have been intensively discussed (Law, C.K., et al. 2000; Chen, Y-C., et al. 2000; Wiiliams, F.A. 1985). Much research has focused on lift flames (Lee, B.J. et al. 1997; Takahashi, F., et al., 1998; Ghosal, S., and Vervisch, L., 2001; Qin, X., et al. 2001; Kim, J., et al., 2002) and edge flames (Ko, Y.S., et al., 2000; Favier, V., and Vervisch, L., 2001; Takagi, T., et al., 2002; Bradley, D., et al., 1996; Chen, R.H., et al., 1992; Shay, M.L., and Ronney, P.D., 1998). The leading edge flame structure is also an important parameter that must be understood in practical systems. Therefore, the interaction of the leading edge flame with an adjunct cold surface has also been investigated (Takahashi, F., et al., 1998; Wichman, I.S., et al., 1999; Daou, R., et al., 2002). The attachment mechanism is a key issue to understanding the flame holding mechanism both in premixed and non-premixed flames. The leading edge of the flame can be regarded as the anchor or stabilizing point. The stabilization point of a laminar flame can be characterized by the local heat release, heat loss, burner dimensions and so on, but there are very few experimental reports about the local equivalence ratio and its relationship to the anchor point of a laminar flame.

The detailed flame structure at an anchor point and its local stoichiometry must be demonstrated experimentally. Chemiluminescence measurements have been performed to illustrate the detailed flame structure both in laminar and turbulent flames (Docquier, N., and Candel, S., 2002; Docquier, N., et al., 2000; Ikeda, Y., et al., 2000; Kojima, J., et al., 2000; Kojima. J., et al., 2003). Typical radicals, such as OH*, CH* and C_2* have been measured, and used to identify the flame front structure and burning velocity of turbulent premixed flames (Yoshida, A., 1988; Adel-Gayed, R.G., et al., 1986; Summerfield, M.,et al., 1955; Samaniego, J.M., et al., 1995). The local flame-front structures in fundamental premixed flames have also been investigated experimentally for laminar (Yoshida, A., 1988; Sinibaldi, J.O., et al., 1998; Chen, J.H., and Im, H.G., 1998; Louch, D.S., and Bray, K.N.C., 1998) and turbulent flames (Adel-Gayed, R.G., et al., 1986) and flame structures at high pressures have been recorded (Kobayashi, K., and Kawazoe, H., 2000; Kobayashi, K., et al., 1998; Ikeda, Y., et al., 2002). However, there are still many unknown parameters that are required for a complete understanding of the leading edge flame structure.

Recent experimental and theoretical studies have investigated several meaningful quantitative correlations between the chemiluminescent emission intensities and the flame structure parameters (Roby, R.J., et al., 1998). Moreover, the OH* spectra profile has been correlated to the flame temperature (Lee, G.J, et al., 2000). The spatial distribution of the vibrational temperature has also been obtained with a conventional two-line method using the C_2* swan emission band in preheated air-hydrocarbon flames (Walsh, K.T., et al., 1998). However, chemiluminescence measurements based on optical techniques are required for combustion control and detailed combustion modelling (Docquier, N., et al., 2000; Walsh, K.T., et al., 1998; Walsh, K.T., et al., 2000; Berg, P.A., et al., 2000). Therefore, a new optical measurement technique was developed using a specially designed Cassegrain optics system to detect local flame emissions (Ikeda, Y., et al., 2000; Kojima, J., et al., 2000; Ikeda, Y., et al., 2002; Akamatsu, F., et al., 1999). Cassegrain optics has a high spatial resolution of less than eighty micrometers in diameter. The system can be used to examine the local OH*, CH* and C_2* chemiluminescence to determine the structure of a premixed flame front; this is an original and valuable approach. Our previous study demonstrated that the emission intensity ratios of OH*/CH* and C_2*/CH* measured at the local flame front were good markers of the equivalence ratio under atmospheric and high-pressure conditions (Ikeda, Y., et al., 2000; Kojima, J., et al., 2000; Ikeda, Y., et al., 2002). The correlation of the OH*, CH* and C_2* emission intensity ratios to the local equivalence ratio in the spatially resolved reaction zone was used to investigate the chemistry and stoichiometry in the stabilization region of laminar flames.

The purpose of this study was to obtain spatially and spectrally resolved chemiluminescent spectra in the leading edge region of a laminar premixed propane/air flame by measuring the local flame emission with a Cassegrain optics system to better understand the flame front Temperature, its location, anchor point location, and flame structure, as well as the stoichiometry and attachment mechanisms of a laminar premixed flame.

2. EXPERIMENTAL DESCRIPTION

The experimental setup is shown in Fig. 1. A Bunsen burner (inner diameter: 12 mm) was installed in open air conditions. A propane/air gas mixture was supplied to the burner nozzle and controlled by a mass flow controller (Kojima Instruments Inc., Air: Model 3200-1/4-AIR-10SLM, Propane: Model 3200-1/4-CH4-1.5SLM) to within 0.3% at full scale. The air flow was fixed at 1.17×10^{-4} m^3/s, and the propane flow was varied between 4.4×10^{-6} and 7.3×10^{-6} m^3/s, over which the equivalence ratio f varied between 0.9 and 1.5. It was not possible to have a stable flame for the lower equivalence ratio under these conditions. Room temperature air was supplied from the bottom of the chamber. A CCD video camera was used to observe the flame.

The local chemiluminescence measurement system is also shown in Fig. 1. Cassegrain optics was used to collect the local flame emissions at the flame front (Ikeda, Y., et al., 2000; Kojima, J., et al., 2000; Ikeda, Y., et al., 2002; Akamatsu, F., et al., 1999). These were comprised of an optical UV grade fiber (core diameter = 100 μm, N.A. = 0.2) and a pair of optimized mirrors: one concave (d = 200 mm), and one convex (d = 80 mm). The Cassegrain optics provided a high spatial resolution by minimizing the spherical aberration of the pair of mirrors and avoiding chromatic aberration. The theoretical spatial resolution of the optics was estimated using ray tracing. The effective control volume was defined using the measured relative intensity rate, with a threshold level of e^{-2} times the peak value. The control volume was estimated to be 80 μm in diameter, which was sufficient to detect spatially resolved flame emissions in the premixed flame fronts. In order to minimize the effect of background light, a mask with a 10-mm slit was mounted on the front mirror.

The collected flame emissions were guided to a grating monochromator (Oriel, MS257) through the optical fiber. A CCD detector coupled to an image intensifier (Andor, DH520) and two different gratings (300 and 2400 lines/mm) were used in the monochromator. The wavelength resolutions of the respective gratings were 0.22 and 0.025 nm. The gain of the image intensifier was maintained at a constant value for each measurement. The exposure time of the CCD detector was 0.2 ms.

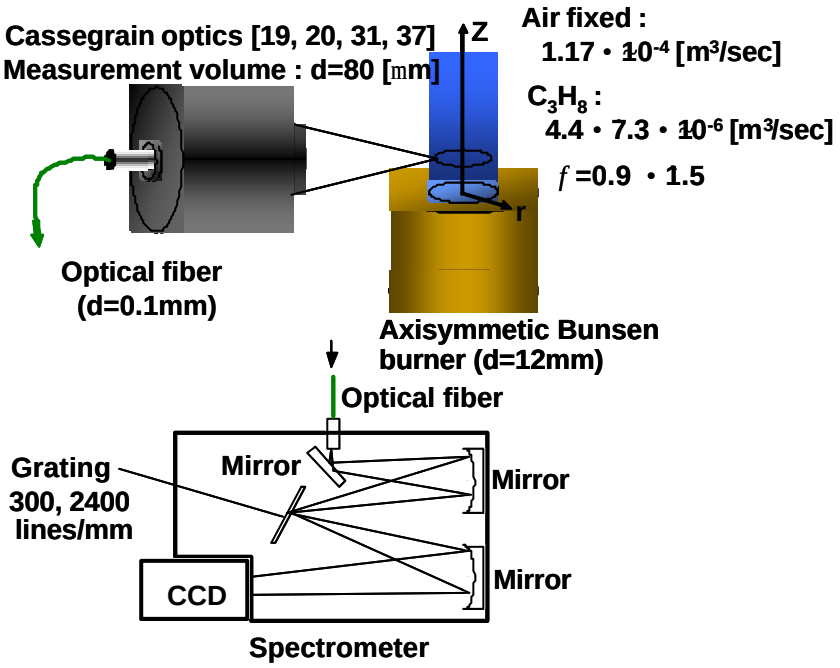

Fig. 1 Schematic layout of experimental apparatus: Bunsen burner (Inner diameter 12 mm), monochromator (grating: 300 and 2400 lines/mm)

3. RESULTS AND DISCUSSION

Figure 2 shows a direct picture of the flame. The burner diameter was 12 mm. The anchor point was located 0.3 to 0.5 mm above the rim, at r = 6.5 mm. The local CH* intensity distribution, measured by the Cassegrain optics system, is also shown in the same figure. The flame front location measured by the Cassegrain optics system was the same as that measured by the CCD camera. The flame front structure, attachment angle, location, and stoichiometry are of particular interest in this study.

Figure 3 shows the local flame spectra at the cone as a function of the height (z = 4 mm, 1 mm, and the anchor point). These were obtained using f = 1.1 and a 300-lines/mm grating. The spectra were measured at the CH* maximum intensity location, which could be determined at a resolution of 100 microns in the z direction. The anchor point was located at the closest position, where the chemiluminescence intensities could not be detected. The chemiluminescence intensities of OH*, CH* and C_2* had the same peaks at all locations. The OH* intensities at z = 1 and 4 mm were almost the same, while the CH* intensity at z = 1 mm was two-thirds of that at z = 4 mm. These intensities decreased dramatically at the anchor point. There was also no remarkable C_2* intensity at the anchor point. Typical emission bands of OH*(0, 0) and CH*(0, 0) were clearly observed within the continuous background CO-O* emissions. The CO-O* (CO_2*) emitters were characterized by a broadband emission spectrum, extending from 300 to 600 nm with no apparent band structure. These were caused by the radiative recombination of CO with atomic oxygen (Gaydon, A.G., 1974). The lower plot shows the detailed flame spectra at the anchor point for different equivalence ratios. The OH* and CH* intensities at f = 0.9 were extremely weak compared to those obtained with a higher equivalence ratio. The strongest emission intensities were measured at f = 1.1. The anchor point for these three conditions shifted slightly, which will be discussed later in the text. These results demonstrated that the local chemluminescence spectra could be measured at a standard flame front (z = 4 mm) and close to the leading edge, that is, the anchor point.

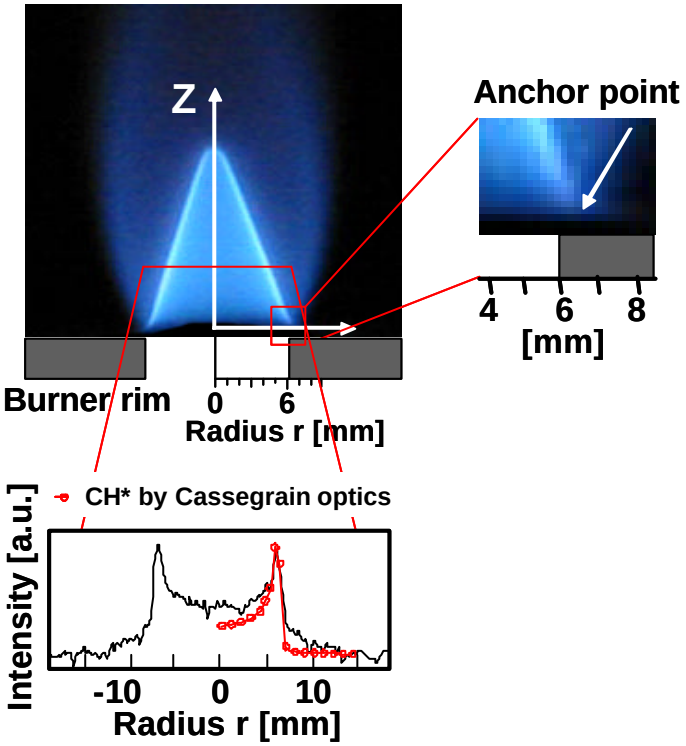

Fig. 2 Direct picture of laminar propane/air premixed flame, set up equivalence ratio was 1.1

Figure 4 gives the anchor point location as a function of the equivalence ratio. The local point measurements were performed at a 100-micron resolution in the z direction and a 50-micron resolution in the *r* direction. The anchor point locations for different equivalence ratios were not the same, and the equivalence ratio location trace was a V shape. The anchor point near $f = 1.0$ was the lower-most point, located at $r = 6.75$ mm and $z = 0.3$ mm, while the anchor point for the lean flame was at a smaller radius and higher location and the anchor point for the rich flame was at a larger radius and higher location. In these tests, the air flow was fixed while the propane flow was varied so that the total flow rate changed. The anchor point of the lean flame was located towards the inner side due to the small flow rate and the heat balance with the cool metal rim. In comparison, the rich flame had a faster flow rate and flame propagation speed. These results can be explained by the flame speed diagram for different equivalence ratios, which shows that the maximum flame speed occurs near $f = 1.0$, while flames in lean or rich conditions are slower.

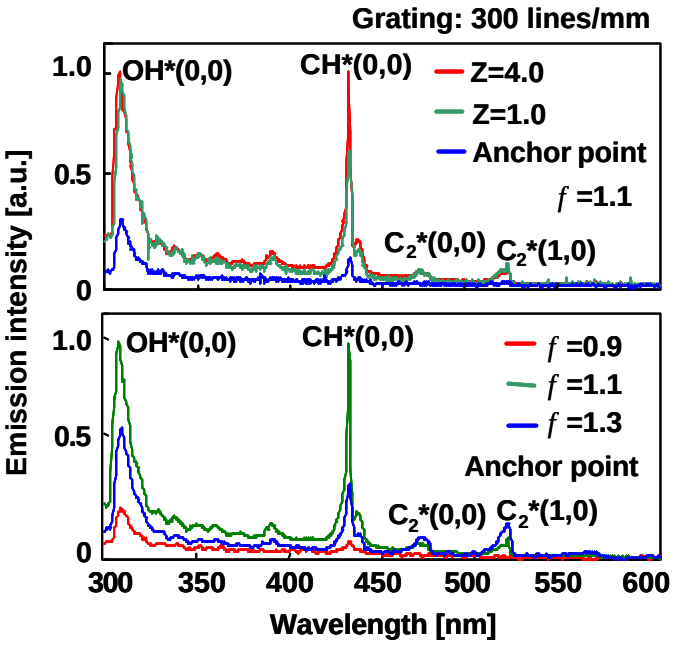

Fig. 3 Flame spectrum at different flame height at f=1.1 and different f at anchor point

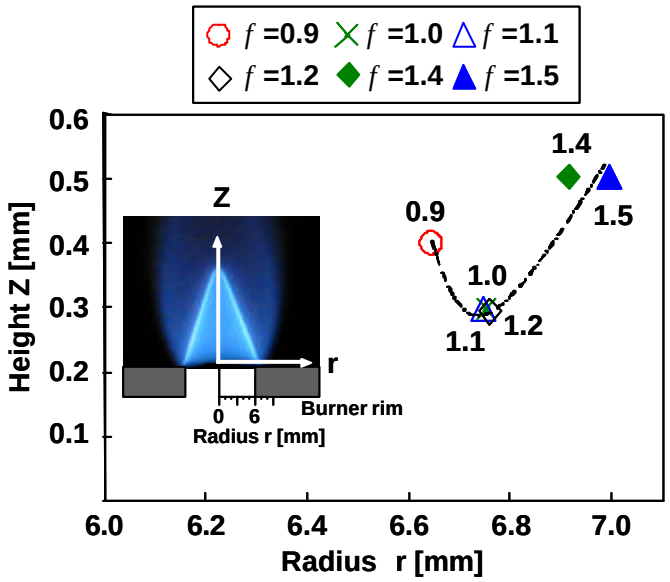

Fig.4 Anchor point location for different equivalence ratio

More details of the flame structure at the anchor point can be observed from the flame spectra. In our previous study, the chemiluminescent emission intensity ratios of OH*/CH*, C_2*/OH* and C_2*/CH* were identified as good markers for detecting the local equivalence ratio in a premixed laminar flame front (Kojima, J., et al., 2000; Ikeda, Y., et al., 2002; Walsh, K.T., et al., 1998). Furthermore, the chemiluminescence intensity ratio of OH*/CH* was less dependent on the pressure, even though the individual chemiluminescence intensities changed with the pressure (Ikeda, Y., et al., 2002). Figure 5 shows the relationship between these intensity ratios and the equivalence ratio. The three emission intensities were measured carefully, and the detailed flame spectra shown in Fig. 3 at z = 4 mm were obtained. These results demonstrated that the local flame equivalence ratio could be determined from the three emission intensity ratios, as reported in our previous papers (Ikeda, Y., et al., 2000; Ikeda, Y., et al., 2002). The intensity ratio of OH*/CH* at the anchor point is superimposed on the same figure using black circles. The intensity ratio of the anchor point was almost constant for different equivalence ratios, even though the anchor point shifted outside the flame in rich conditions, as shown in Fig. 4.

The flame structure at the anchor point should be based on the same chemical processes, regardless of the equivalence ratio. To demonstrate this, the detailed flame spectra of OH* for different equivalence ratios were compared to those measured at a standard flame front (z = 4 mm) in Fig. 6. The upper plots show the spectra that were measured at z = 4 mm, and the lower plots show the spectra that were measured at the anchor point. The left-hand side spectra were normalized using the OH*(0, 0) P-branch peak. The detailed OH* spectrum had much fewer discrepancies between different equivalence ratios, both at z = 4 mm and at the anchor point. The OH*(0, 0) R-branch peak of the f = 0.9 curve was slightly lower than the curves for f = 1.1 and 1.3. There were heat balances at the anchor point to provide sufficient heat loss to the attached metal surface. These can decrease the flame temperature, especially at low equivalence ratios. The temperature can be measured from the detailed OH* spectra, as demonstrated by plasma diagnostics (Laux, C.O., et al., 2003). This will be investigated later in the text. A comparison of the detailed OH* spectra at different equivalence ratios proved that the chemistry at the anchor point was the same for each condition, but the temperature or heat loss varied. We will see this effect in more detail later in the text.

Figure 7 gives the flame front locations near the burner rim for different equivalence ratios. The anchor points for each equivalence ratio were shown in Fig. 4; these were used to determine the flame front location and its shape close to the attachment rim. The detailed flame spectra were measured with a 50-micron resolution in the r direction at different heights, and the CH* peak location was used to identify the flame front location. As shown in the figure, the shape of the flame front had a wider angle closer to the rim. The location of the anchor point was close to the metal rim at lower equivalence ratios, and it shifted outwards as the equivalence ratio increased. The height of the anchor point also increased slightly with the equivalence ratio. The anchor points for f = 0.9 to 1.2 were at the same location, which was also the location observed in Fig. 4. The flame front shifted a distance of about 200 microns in the r direction and 100 microns in the z direction over the range of equivalence ratios.

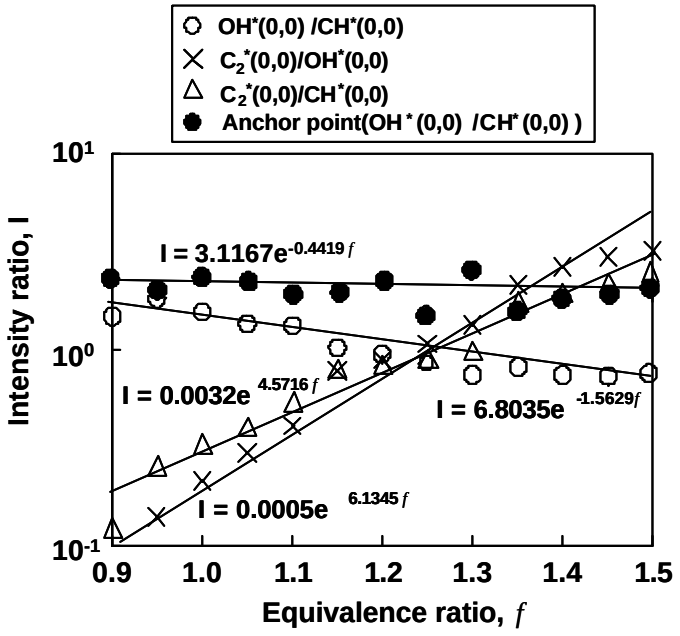

Fig. 5 Relationship of emission intensities with equivalence ratio

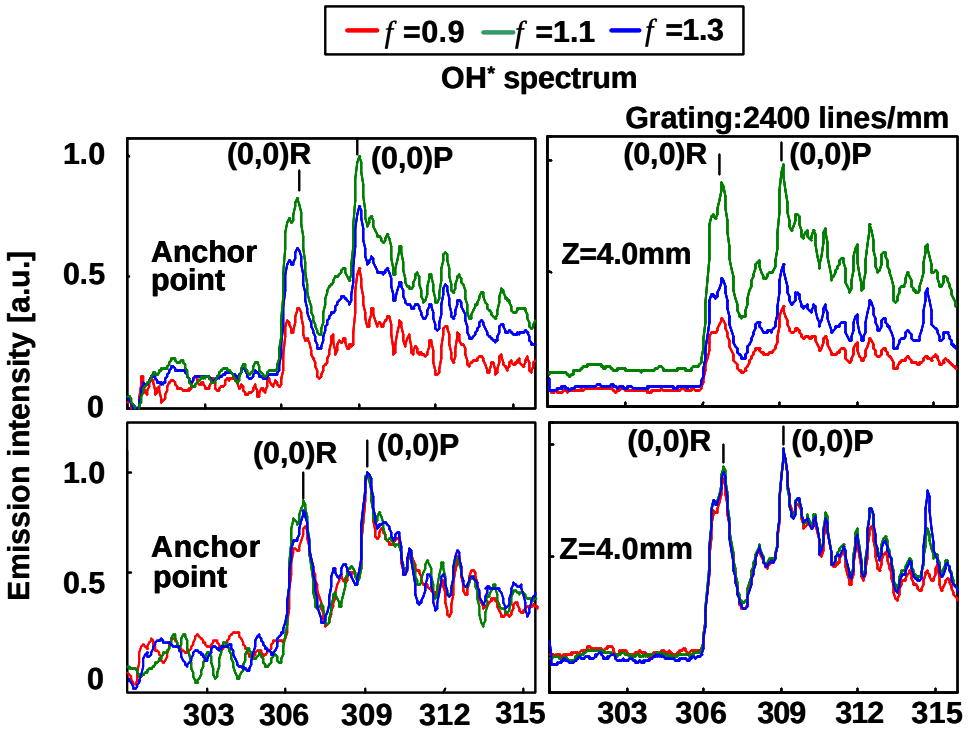

Fig. 6 Detail flame spectra in OH and CH* band at equivalence ratio*

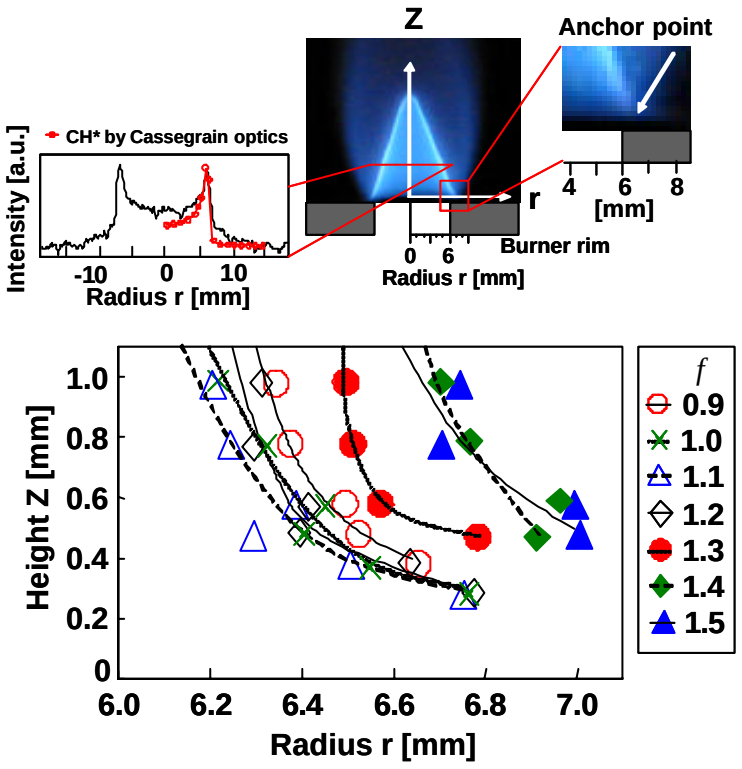

Fig. 7 Flame front location and anchor point for different equivalence ratio

The flame front location and its structure close to the rim at different equivalence ratios was not the same, but the stoichiometry at the anchor point remained similar, as shown in Fig. 8. This result indicated that the flame structure and chemistry at the anchor point were almost entirely dominated by the same chemical reaction mechanisms. At z = 1.0 mm, the flame front location moved outwards as the equivalence ratio increased. The local equivalence ratios at the flame front when f = 0.9 to 1.2 did not change at z = 0.5 mm, but when z = 0.2 mm, the local equivalence ratios decreased to between 0.7 to 0.9. For the rich flame with f = 1.5, the local equivalence ratio decreased to 0.7 at z = 0.5 mm. It was found that at the anchor point the flame front location and its structure for different equivalence ratios did not change; it remained at a constant value and constant location.

The temperature at the anchor point cannot be measured directly. Therefore, we used the detailed OH* peak ratio to determine the temperature, as demonstrated by plasma diagnostics (Laux, C.O., et al., 2003). As shown in Fig. 6, the detailed OH* spectra were used to compare the peak intensities for different equivalence ratios, which were functions of the rotational temperature. The intensity ratio of the OH* (0, 0) R-branch and (0, 0) P-branch are compared in Fig. 9. The P/R intensity ratios had less discrepancies in the flame when z = 0.7 mm for different equivalence ratios, which indicated that the flame temperature at those conditions was relatively constant. On the other hand, the P/R intensity ratio at the anchor point varied from 0.78 to 0.86 for f = 0.9 to 1.5. These results demonstrated that the flame temperature at the anchor point was not the same for different equivalence ratios. We cannot provide an accurate estimate of the flame temperature from this experiment, but the flame front location and its structure were measured with sufficient resolution.

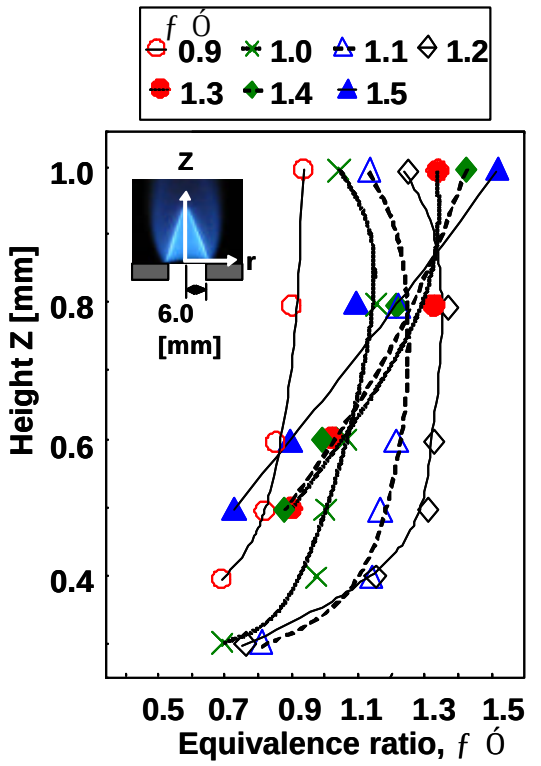

Fig. 8 Equivalence ratio change near anchor point

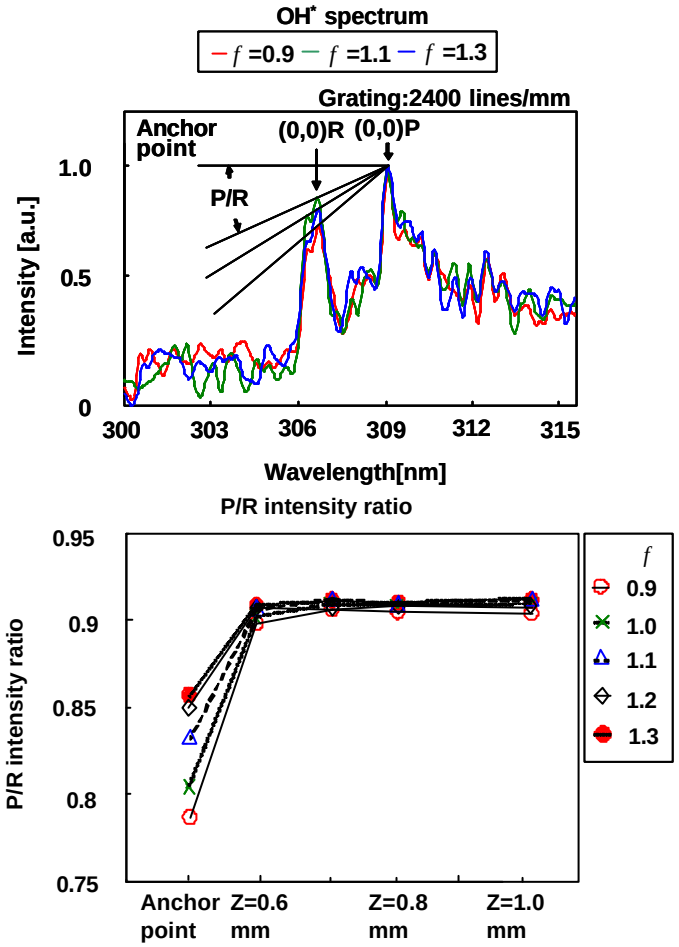

Fig. 9 Temperature estimation using detailed OH R and P branch intensity ratio*

4. CONCLUSIONS

Spatially and spectrally resolved chemiluminescence spectra of premixed laminar propane/air flames were measured in open air conditions. The spatially resolved chemiluminescence measurements were successfully performed at the flame front and the anchor point locations for different equivalence ratios using a Cassegrain optics system. The anchor point location and the flame structure were successfully determined from the detailed flame spectra. The anchor point trace was a V shape, with the lower anchor point location at 0.3 mm in the z direction and 6.8 mm in the r direction. The equivalence ratios of the anchor points were calculated using the relationship between the OH* and CH* intensity ratios and the local equivalence ratio obtained at the standard flame front ($z = 4$ mm). The values were almost constant between 0.7 and 0.8 for various equivalence ratios. The location of the anchor point moved outwards and increased in height with the equivalence ratio, but the chemical processes at the anchor point were similar. The equivalence ratio of the flame remained at a constant value when $z = 0.5$ mm, but it changed drastically close to the attachment rim. When $f = 1.5$, the equivalence ratio decreased to 0.7 at $z = 0.5$ mm. The temperature of the anchor point, estimated from the OH* R and P branch peak intensity ratios, suggested that the flame temperature for various equivalence ratios remained relatively constant at the flame front but changed considerably at the anchor point.

ACKNOWLEDGMENTS

Authors thank to Mr. Nakayama of Okayama University for his technical assistance in the measurement.

REFERENCES

Adel-Gayed, R.G., Bradley, D., Lawes, M., and Lung, F.K-K (1986) Proc. Combust. Inst. 21, pp.497.

Akamatsu, F., Wakabayashi, T., Tsushima, S., Katsuki, M., Mizutani, Y., Ikeda, Y., Kawahara, N., and Nakajima, T. (1999) Meas. Sci. Technol. 10, pp.1240.

Berg, P.A., Hill, D.A., Noble, A.R., Smith, G.P., Jefferies, J.B. and Crosley, D.R. (2000) Combust. Flame 121, pp.223..

Bradley, D., Gaskell, P.H., Kwan, K.C., and Scott, M.J.(1996) "Two-Dimensional Mathematical Modeling of Laminar Premixed, Methane-Air Combustion on an Experimental Slot Burner", Proc. Combust. Inst. 26, pp.915-921.

Chen, J.H., and Im, H.G. (1998) Proc. Combust. Inst. 27, pp.819.

Chen, R.H., Mitchell, G.B., and Ronney, P.D. (1992) "Diffusive-Thermal Instability and Flame Extiction in Nonpremixed Combustion", Proc. Combust. Inst. 24,pp.213.

Chen, Y-C., Bilger, R.W. (2000) "Stabilization Mechanisms of Liquid Laminar Flames in Axisymmetric Jet Flow", Combust. Flame 123; pp.23-45.

Daou, R., Daou, J., and Dold, J. (2002) "Effect of Volumetric Heat Loss on Triple-Flame Propagation", Proc. Combust. Inst. 29, pp.1559-1564.

Docquier, N., Belhalfaoui, S., Lacas, F., Darabiha, N., and Rolon, C. (2000) "Experimental and Numerical Study of Chemiluminescence in Methane/Air High-Pressure Flames for Active Control Applications", Proc. Combust. Inst. 28, pp.1765-1774.

Docquier, N., and Candel, S. (2002) "Combustion Control and Sensors: A Review", Prog. In Energy and Combust. Sci. 28, pp.107-150.

Favier, V., and Vervisch, L. (2001) "Edge Flames and Partially Premixed Combustion in Diffusion Flame Quenching", Combust. Flame 125, pp.788-803.

Gaydon, A.G. (1974) "The Spectroscopy of Flames (2nd ed)", Chapmann and Hall, London.

Ghosal, S., and Vervisch, L. (2001) "Stability Diagram for Lift-Off and Blowout of a Round Jet Laminar Diffusion Flame", Combust. Flame 123, pp.646-655.

Ikeda, Y., Kojima, J., Nakajima, T., Akamatsu, F., and Katsuki, M. (2000) "Measurement of the Local Flamefront Structure of Turbulent Premixed Flames by Local Chemiluminescence", Proc. Combust. Inst. 28, pp.343-350.

Ikeda, Y., Kojima, J., and Hashimoto, H. (2002) "Local Chemiluminescence Spectra Measurements in a High-Pressure Laminar Methane/Air Premixed Flame", Proc. Combust Inst. 29, pp.1495-1501.

Kim. J., Won, S.H., Shin, M.K., and Chung, S.H. (2002) "Numerical Simulation of Oscillating Lifted Flames in Coflow Jets with Highly Diluted Propane", Proc. Combust. Inst. 29, pp.1589-1595.

Ko, Y.S., Chung, S.H., Kim, G.S., and Kim, S.W. (2000) "Stoichiometry at the Leading Edge of a Tribrachial Flame in Laminar Jets from Raman Scattering Technique", Combust. Flame 123, pp.430-433.
Kobayashi, K., Kawabata, Y., and Maruta, K. (1998) Proc. Combust Inst. 27, pp.941.

Kobayashi, K., and Kawazoe, H. (2000) Proc. Combust Inst. 28, pp.375.

Kojima, J., Ikeda, Y., and Nakajima, T. (2000) "Spatially Resolved Measurement of OH*, CH*, and C_2* Chemiluminescence in the Reaction Zone of Laminar Methane/Air Premixed Flames", Proc. Combust. Inst. 28, pp.1757-1764.

Kojima. J., Ikeda, Y., and Nakajima, T. (2003) "Multi-Point Time-Series Observation of Optical Emissions for Flame-Front Motion Analysis", Meas. Sci. Technol. 14, pp.1714-1724.

Laux, C.O., Spence, T.G., Kruger, C.H., and Zare, R.N. (2003) "Optical Diagnostics of Atmospheric Pressure Air Plasmas", Plasma Source Sci. Technol. 12, pp.125-138.

Law, C.K., Sung, C.J. (2000) "Structure, Aerodynamics, and Geometry of Premixed Flamelets", Prog. In Energy and Combust. Sci. 26; pp.459-505.

Lee, B.J., Chung, S.H. (1997) "Stabilization of Lifted Tribrachial Flames in a Laminar Nonpremixed Jet", Combust. Flame 109, pp.163-172.

Lee, G.J, Kim, K. and Santavicca, A.D. (2000) Proc. Combust Inst. 28, pp.415.

Louch, D.S., and Bray, K.N.C. (1998) Proc. Combust. Inst. 27, pp.801.

Qin, X., Puri, I.K. and Aggarwal, S.K. (2002) "Characteristics of Lifted triple Flames Stabilized in the Near Field of a Partially Premixed Axisymmetric Jet", Proc. Combust. Inst. 29, pp.1565-1572.

Roby, R.J., Reaney, J.E., Johnsson, E.L. (1998) Proc. International Joint Power Generation Conference 1, pp.593.

Samaniego, J.M., Egolfopoulos, F.N., and Bowman, C.T. (1995) Combust. Sci. and Tech. 109, pp.183.

Shay, M.L., Ronney, P.D. (1998) "Nonpremixed Edge Flames in Spatially Varying Straining Flows", Combust. Flame 112, pp.171-180.

Sinibaldi, J.O., Mueller, C.J., and Driscoll, J.F. (1998) Proc. Combust. Inst. 27, pp.827.

Summerfield, M., Riter, S.H., Kebely V. and Mascolo R.W. (1955) Jet Propulsion 25, pp.377.

Takagi, T., Nakajima, I., and Kinoshita, S. (2002) "Structure and Propagation of Strain-Controlled H_2/N_2/Air Diffusion Edge Flames", Proc. Combust. Inst. 29, pp.1573-1579.

Takahashi, F., Schmoll, W.J., and Katta, V.R. (1998) "Attachment Mechanisms of Diffusion Flames", Proc. Combust. Inst. 27, pp.675-684.

Walsh, K.T., Long, M.B. Tanoff, M.A. and Smooke M.D. (1998) Proc. Combust. Inst. 27, pp.615.

Walsh, K.T., Long, M.B., Smooke, M.D., Luque, J., Jefferies, J.B., Smith, G.P. and Crosley, D.R. (2000) Combust. Flame 122, pp.172.

Wichman, I.S., Pavlova, Z., Ramadan, B., and Qin, G. (1999) "Heat Flux from a Diffusion Flame Leading Edge to an Adjacent Surface", Combust. Flame 118, pp.651-668.

Williams, F.A. (1985) "Combustion Theory", 2nd Ed. Addison-Wesley Publishing Company, USA.

Yoshida, A. (1988) Proc. Combust. Inst. 22, pp.1471.